Available online at www.sciencedirect.com

ScienceDirect

Procedia Structural Integrity 13 (2018) 753–762

Structural Integrity Procedia

www.elsevier.com/locate/procedia

ECF22 - Loading and Environmental effects on Structural Integrity

Hydrogen Embrittlement in Advanced High Strength Steels and Ultra High Strength Steels: a new investigation approach

Antonello Cherubini, Linda Bacchi, Serena Corsinovi, Marco Beghini, Renzo Valentini

University of Pisa, Largo Lucio Lazzarino 2, Pisa, Italy

Abstract

In order to reduce CO_2 emissions and fuel consumption, and to respect current environmental norms, the reduction of vehicles weight is a primary target of the automotive industry. Advanced High Strength Steels (AHSS) and Ultra High Strength Steel (UHSS), which present excellent mechanical properties, are consequently increasingly used in vehicle manufacturing. The increased strength to mass ratio compensates the higher cost per kg, and AHSS and UHSS are proving to be cost-effective solutions for the body-in-white of mass market products.

In particular, aluminized boron steel can be formed in complex shapes with press hardening processes, acquiring high strength without distortion, and increasing protection from crashes. On the other hand, its characteristic martensitic microstructure is sensitive to hydrogen delayed fracture phenomena and, at the same time, the dew point in the furnace can produce hydrogen consequently to the high temperature reaction between water and aluminum. The high temperature also promotes hydrogen diffusion through the metal lattice under the aluminum-silicon coating, thus increasing the diffusible hydrogen content. However, after cooling, the coating acts as a strong barrier preventing the hydrogen from going out of the microstructure. This increases the probability of delayed fracture. As this failure brings to the rejection of the component during production, or, even worse, to the failure in its operation, diffusible hydrogen absorbed in the component needs to be monitored during the production process.

For fast and simple measurements of the response to diffusible hydrogen of aluminized boron steel, one of the HELIOS innovative instruments was used, HELIOS II. Unlike the Devanathan cell that is based on a double electrochemical cell, HELIOS II is based on a single cell coupled with a solid-state sensor. The instrument is able to give an immediate measure of diffusible hydrogen content in sheet steels, semi-products or products, avoiding time-consuming specimen palladium coating with a guided procedure that requires virtually zero training.

Two examples of diffusible hydrogen analyses are given for Usibor®1500-AS, one before hot stamping/ quenching, and one after hot stamping, suggesting that the increase in the number of dislocations during hot stamping could be the main responsible for the lower apparent diffusivity of hydrogen.

© 2018 The Authors. Published by Elsevier B.V.
Peer-review under responsibility of the ECF22 organizers.

Keywords: Hydrogen; HE; HSSA; Advanced High Strength Steel; Desorption; HELIOS;

* Corresponding author: Renzo Valentini
E-mail address: renzo.valentini@unipi.it

2452-3216 © 2018 The Authors. Published by Elsevier B.V.
Peer-review under responsibility of the ECF22 organizers.
10.1016/j.prostr.2018.12.125

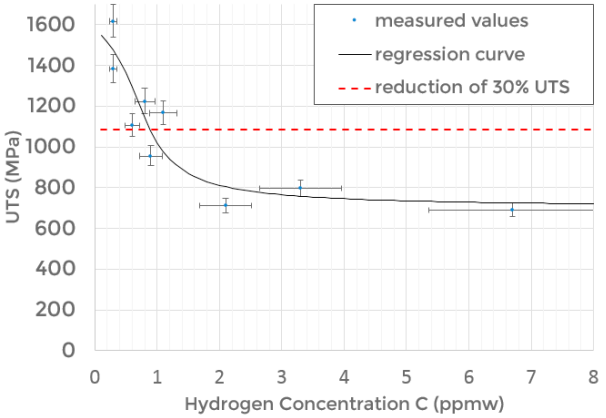

Fig. 1. Mechanical performance of Usibor®1500-AS vs concentration of diffusible hydrogen. Picture from Tedesco et al. (2017).

Fig. 2. Left: the Cassino plant of Fiat Chrisler Automobiles, where the tests have been carried out. Right: after, hydrogen charging, the Usibor®1500-AS cracked at the yield strength, well below its original hydrogen-free resistance. The crack is several centimeters long and is highligthed by the red arrow. Pictures courtesy of FCA.

1. Introduction

In recent years, the automotive sector is increasingly demanding materials with higher strength to mass ratio. The main reason for this is represented by more severe regulations in terms of CO_2 emissions and safety, which, in turn, translates to a reduction in fuel consumption and vehicle mass. As a result, stamping of hot sheets in cooled dies is being spread in the manufacturing of the car body-in-white (Merklein et al. (2016)) and, also, the industry is shifting from Low Carbon (LC) steels to materials with higher mechanical performances such as High Speed Steels (HSS), Advanced High Strength Steels (AHSS), and Ultra High Strength Steel (UHSS) . For example from year 2000 to 2016 Fiat Crysler Automobiles has increased its share of HSS and UHSS from 27% to 61% and, at the same time, it has reduced its share of low carbon steel from 73% to 21% (Tedesco et al. (2017)).

In this scenario, the present work aims at investigating the fundamental mechanism that is responsible for longer permeation times after hot stamping in Aluminium-Silicon coated Usibor®1500-AS

Per meglio calibrare questi strumenti (che fanno le misure veloci) occorre conoscere bene l'intrappolamento di idrogeno in questi acciai e ci metto il modello numero di permeazione e un esempio di calcolo di trappole sull'usibor.

cricca evidenziata durante i test fatti a cassino

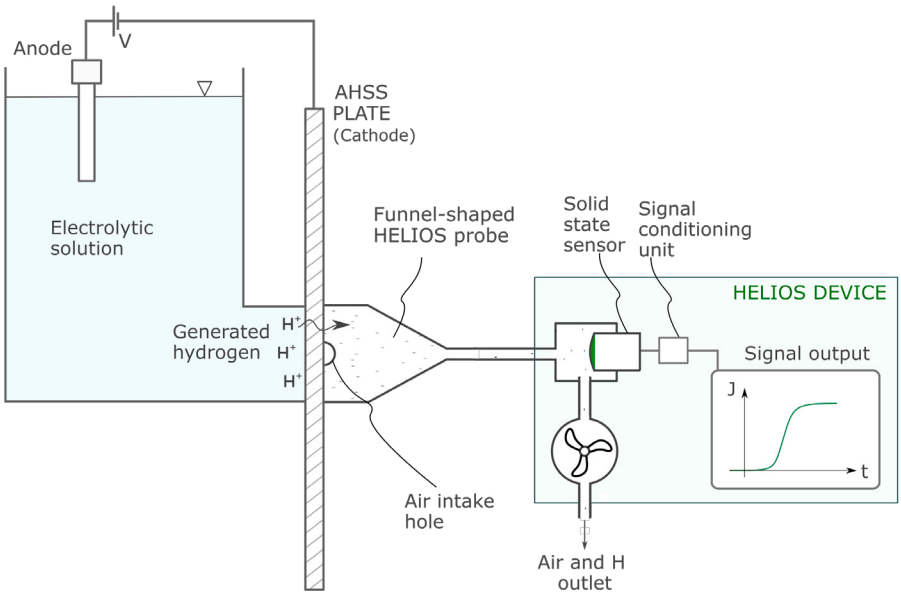

Fig. 3. The permeation test setup based on solid state hydrogen sensor, performed with the HELIOS device.

quel pezzo aveva la concentrazione di idrogeno superiore alla quella stimata critica(stimata con gli ssrt)
la cricca partita a snervamento

2. Experimental setup

The experimental setup is shown in Fig. 3. An electrolytic cell is used to generate hydrogen on the left surface of the AHSS plate. The hydrogen naturally diffuses through the steel sheet and it flows out of the right side where it goes into a funnel-shaped probe that is continuously drawing air. The mixture air-hydrogen is then analyzed inside the HELIOS device by a solid state sensor that measures the hydrogen concentration and is connected to the acquisition electronics.

Comparing to a standard Devanathan cell, the HELIOS measurement does not require palladium coated specimens, thus it allows faster and less expensive measurements. On the other hand, the accuracy is comparable to that of a Devanathan cell, provided that the solid state sensor is calibrated beforehand.

In this work, this experimental setup was used to analyze the hydrogen permeation of a plate of cold rolled, quenched, un-coated, high performance USIBOR2000® before undergoing hot stamping. According to its Datasheet (2018), the USIBOR2000® has UTS $\geq$ 1800 MPa and YS $\geq$ 1400 MPa.

3. Modelling diffusion of hydrogen in steels

We model hydrogen permeation in steel as a monodimensional diffusion problem where hydrogen moves through the material lattice and its motion is adversely affected by the presence of traps such as crystallographic imperfections, dislocations, grain boundaries, precipitates, etc. We assume that the traps saturate according to the non-linear diffusion model presented in McNabb et al. (1963) and we assume that there are only two types of traps: reversible or irreversible, meaning that they are able or are not able to release the hydrogen that they have trapped. The equations are therefore:

$$\begin{cases} \dfrac{\partial C}{\partial t} = D\dfrac{\partial^2 C}{\partial x^2} - N_r\dfrac{\partial v}{\partial t} - N_i\dfrac{\partial w}{\partial t} \\ \dfrac{\partial v}{\partial t} = K_r C\,(1-v) - pv \\ \dfrac{\partial w}{\partial t} = K_i C\,(1-w) \end{cases} \tag{1}$$

The first equation models the hydrogen diffusion as a Fick diffusion to which the two trapping terms are added. In this equation C is the hydrogen concentration in the lattice expressed in (atoms/m^3), D is the diffusion coefficient of hydrogen in pure iron (m^2/s), N_r and N_i are the concentrations of reversible and irreversible traps respectively (atoms/m^3), v is the fraction of occupied reversible traps (non dimensional quantity between 0 and 1) and w is the fraction of occupied irreversible traps (non dimensional quantity between 0 and 1). Finally t and x represent time (s) and space (m) (thickness).

The second equation represent the saturation law of reversible traps that is composed by the sum of two terms, the trapping term (proportional to the fraction of free reversible traps $1 - v$) and the release term (proportional to the fraction of occupied reversible traps v). In this equation k_r is the trapping rate of reversible traps (m^3/(atoms s)) and p is the release rate of reversible traps (1/s).

Similarly, the third equation models the saturation law of irreversible traps, and in this equation k_i is the trapping rate of irreversible traps (m^3/(atoms s)) and the there is no release rate of irreversible traps which is zero by definition of irreversible.

The hydrogen diffusion terms C, v and w are functions of space and time and a less synthetic formal expression for each of them would be $C(x,t)$, $v(x,t)$ and $w(x,t)$, while D, N_r, N_i, K_r, K_i and p are material properties and are functions of space only and we can also write them as $D(x)$, $N_r(x)$, $N_i(x)$, $K_r(x)$ $K_i(x)$ and $p(x)$.

The hydrogen flow that is coming out of the outlet side is found according to Fick's first law, by means of the following expression:

$$J = -D\,(a)\left.\frac{\partial C}{\partial x}\right|_{x=a} \tag{2}$$

where a is the plate thickness.

4. Modelling hydrogen permeation through a planar plate

In the specific case of a hydrogen permeation test performed on the rolled AHSS plate described in Section 2, the diffusion model described in section 3 can be applied with the following additional hypotheses:

- The material is assumed to be homogeneous and without any surface coating, therefore the material properties D, N_r, N_i, K_r, K_i and p can be assumed to be constant in time and space.

- The initial conditions are as follows:

$$\begin{cases} C(x,0) = 0 \\ C(0,t) = C_0 \\ C(a,t) = 0 \\ v(x,0) = 0 \\ w(x,0) = 0 \end{cases} \tag{3}$$

where the coordinates of the inlet and outlet side are $x = 0$ and $x = a$, respectively, a (m) is the plate thickness and C_0 (atoms/m^3) is the hydrogen concentration at the inlet side.

4.1. Solution of the system

In Kiuchi et al. (1983) the diffusion coefficient for BCC iron The lattice diffusion coefficient of hydrogen is computed as in Kiuchi et al. (1983) by means of the following Arrhenius-like equation:

$$D = D_\infty \ \exp\left(\frac{E_a}{RT}\right) \tag{4}$$

where D_∞ is the diffusion coefficient of hydrogen through pure iron at infinite temperature, E_a is the activation energy for hydrogen diffusion, R is the universal gas constant and T is the temperature.

If D is constant along the thickness, the hydrogen flow J at the end of the simulation time should be close to the steady state value of the hydrogen flow $J_\infty = C_0 D/a$

5. Experimental Results

We solved the system of partial differential equations (1) with a finite difference forward-Euler method with fixed time-step dt and fixed space-step dx, that has the advantages of being simple and reliable although these features come with the disadvantages of conditional stability and relatively high computational times (approximately 6 minutes in this case).

The equations that are looped by the solver are here reported for the n-th time step and for the i-th space step:

$$\begin{cases} dv = dt \ \ K_r \, C\,(i,n)\,(1 - v\,(i,n)) - dt\, p\, v\,(i,n) \\ dw = dt \ \ K_i \, C\,(i,n)\,(1 - w\,(i,n)) \\ v\,(i,n+1) = v\,(n,i) + dv \\ w\,(i,n+1) = w\,(n,i) + dw \\ C\,(i,n+1) = C\,(n,i) + D\dfrac{dt}{dx}\dfrac{((C\,(i+1,n) - C\,(i,n))\,/dx) - ((C\,(i,n) - C\,(i-1,n))\,/\,dx)}{/} - N_r\, dv - N_i\, dw \end{cases} \tag{5}$$

D was found with Eq. 4, C_0 was found by means of a calibration of the experimental setup, and the trap parameters were chosen so that the simulated hydrogen flow curve matches the experimental one. The complete list of input parameters is shown in Table **??**.

A convenient one-number measurement of the permeation tests is represented by the effective diffusion coefficient. Four different well-known values for this number are shown in Table **??** and they were computed with the following methods: the '63% ' method that yielded D_{63} on the simulated curve and D_{63x} on the experimental curve, the 'time

lag' method that yielded D_{TL} and D_{TLx}, the 'break through' method (D_{BT} and D_{BTx}) and the 'Fourier' method (D_F and D_{Fx}).

Table 1. **Usibor 1500 BEFORE Hot Stamping.**

Data		
Diffusion coefficient of hydrogen through pure iron at infinite temperature	D_∞	7.23e−08 m^2/s
Diffusion activation energy	E_a	5.69e+03 J/mol
Universal gas constant	R	8.31 $J/(mol\,^\circ K)$
Temperature	T	296.15°K
Lattice diffusion coefficient of hydrogen through AHSS	D	7.16e−09 m^2/s
Hydrogen concentration at the inlet side of the plate	C_0	8.00e+23 $(atoms/m^3)$
Concentration of reversible traps	N_r	7.55e+24 $atoms/m^3$
Trapping rate of reversible traps	K_r	1.17e−24 $m^3/(atoms\ s)$
Release rate of reversible traps	p	3.40e−02 s^{-1}
Concentration of irreversible traps	N_i	5.00e+23 $atoms/m^3$
Trapping rate of irreversible traps	K_i	5.00e−24 $m^3/(atoms\ s)$
Non dimentional ratio	ν/μ	2.75e+01 ()
Binding energy of reversible traps	E_b	41.1 kJ/mol
Effective diffusion coefficient on simulated H flow		
63%	D_{63}	2.76e−10 m^2/s
Time Lag	D_{TL}	2.90e−10 m^2/s
Break Through	D_{BT}	1.33e−10 m^2/s
Fourier	D_F	2.70e−10 m^2/s
Effective diffusion coefficient on experimental H flow		
63%	D_{63x}	2.78e−10 m^2/s
Time Lag	D_{TLx}	2.93e−10 m^2/s
Break Through	D_{BTx}	1.34e−10 m^2/s
Fourier	D_{Fx}	2.86e−10 m^2/s

The results of the experimental tests and the simulations are shown in Figs. 4 and 5. Fig. 4 refers to the Usibor before hot stamping/ quenching, while Fig. 5 to the Usibor after hot stamping/ quenching.

Fig. **??**A shows the time history of the hydrogen flow, J, that is permeating through the AHSS steel plate. The red line was obtained experimentally, while the blue-fading-to-green line was obtained numerically by integrating the system of equations (1). The blue color represents the beginning of the simulation time, while the green color represents the end. The horizontal dashed grey line at the top of the chart show the value of J_∞. The blue text at the top summarizes the valued of the effective diffusion coefficients of the simulated curve. The small circles point to the time and flow used to compute D_{63} and D_{63x}, the small triangles point to the time and flow used to compute D_{TL} and D_{TLx}, and the small squares point to the time and flow used to compute D_{BT} and D_{BTx}. The grey text on the right provides two numerical parameters that get closer to 100% as the simulated curve approaches J_∞.

Fig. **??**B shows the simulated hydrogen concentration, C, along the thickness of the AHSS steel plate. Several lines are printed at different simulation times. The blue color represents the beginning of the simulation, while the green color represents the end.

Table 2. **Usibor 1500 AFTER Hot Stamping.**

Data		
Diffusion coefficient of hydrogen through pure iron at infinite temperature	D_∞	7.23e−08 m^2/s
Diffusion activation energy	E_a	5.69e+03 J/mol
Universal gas constant	R	8.31 $J/(mol\,^\circ K)$
Temperature	T	296.15°K
Lattice diffusion coefficient of hydrogen through AHSS	D	7.16e−09 m^2/s
Hydrogen concentration at the inlet side of the plate	C_0	8.00e+23 $(atoms/m^3)$
Concentration of reversible traps	N_r	2.57e+25 $atoms/m^3$
Trapping rate of reversible traps	K_r	1.05e−24 $m^3/(atoms\ s)$
Release rate of reversible traps	p	3.40e−02 s^{-1}
Concentration of irreversible traps	N_i	5.00e+23 $atoms/m^3$
Trapping rate of irreversible traps	K_i	5.00e−24 $m^3/(atoms\ s)$
Non dimentional ratio	ν/μ	2.47e+01 ()
Binding energy of reversible traps	E_b	40.8 kJ/mol
Effective diffusion coefficient on simulated H flow		
63%	D_{63}	8.93e−11 m^2/s
Time Lag	D_{TL}	9.35e−11 m^2/s
Break Through	D_{BT}	4.30e−11 m^2/s
Fourier	D_F	8.25e−11 m^2/s
Effective diffusion coefficient on experimental H flow		
63%	D_{63x}	9.00e−11 m^2/s
Time Lag	D_{TLx}	9.44e−11 m^2/s
Break Through	D_{BTx}	4.68e−11 m^2/s
Fourier	D_{Fx}	8.45e−11 m^2/s

Fig. **??**C shows the fraction of occupied reversible traps, ν, along the thickness of the AHSS steel plate. Several lines are printed at different simulation times. The color code is the same of Fig. **??**B. The grey dashed lines represent the steady state values of the ν distribution for different values of the non-dimensional parameter $\nu/\mu = K_r C_0/p$.

Finally Fig. **??**D shows the fraction of occupied irreversible traps, w, along the thickness of the AHSS steel plate, similarly to Fig. **??**C. Note that the irreversible traps are saturated at the end of the simulated permeation.

Acknowledgements

The authors would like to thank Dr. XXX from ArcelorMittal for supplying the analyzed material.

References

McNabb, A., Foster, P. K., 1963. A new analysis of the diffusion of hydrogen in iron and ferritic steels, Transactions of the Metallurgical Society of AIME, Vol. 227 (1963), pp. 618-627

K. Kiuchi and R. B. McLellan, The solubility and diffusivity of hydrogen in well-annealed and deformed iron, Acta metal. Vol. 31, 7 (1983), pp. 961-1140

ArcelorMittal, Steels for hot stamping Usibor® and Ductibor®, https://automotive.arcelormittal.com/saturnus/sheets/E_EN.pdf (2018)

Tedesco M.M., DAiuto F., Valentini R., Corsinovi S., Effects of industrial parameters on delayed fracture in hot stamped components, Materials in Car Body Engineering 2017, 16-18 May 2017, Bad Nauheim, Germany (2017)

Merklein M., Wieland M., Lechner M., Bruschi S. and Ghiotti A., Hot stamping of boron steel sheets with tailored properties: A review, Journal of Materials Processing Technology, Vol. 228 (2016), pp. 11-24

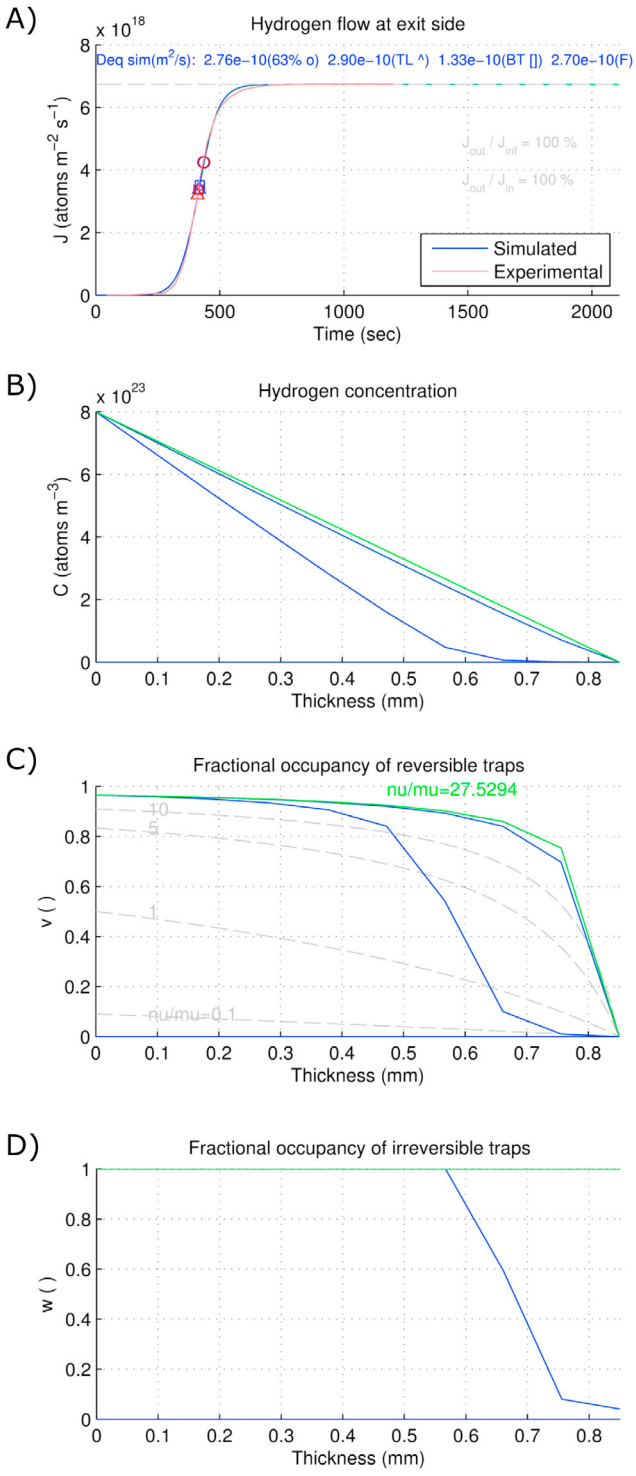

Fig. 4. The results of the permeation analysis performed on the Usibor 1500 BEFORE quenching.

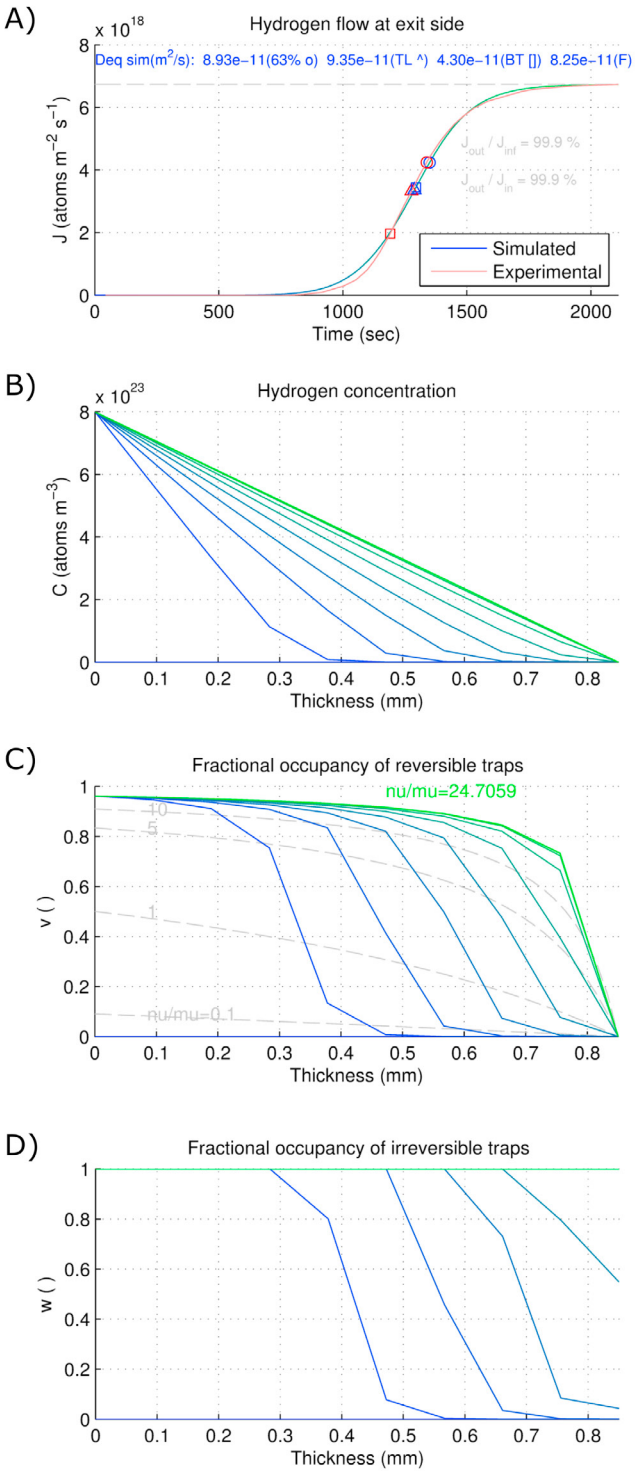

Fig. 5. The results of the permeation analysis performed on the Usibor 1500 AFTER quenching.